

Intrinsic magnetism in monolayer transition metal trihalides: a comparative study

Shalini Tomar,^{1,2} Barun Ghosh,³ Sougata Mardanya,³ Priyank Rastogi,² B. S. Bhadoria,¹ Yogesh Singh Chauhan,² Amit Agarwal,^{3,*} and Somnath Bhowmick^{4,†}

¹*Department of Physics, Bundelkhand University, Jhansi 284128, India*

²*Department of Electrical Engineering,
IIT Kanpur, Kanpur 208016, India*

³*Department of Physics, Indian Institute of Technology, Kanpur 208016, India*

⁴*Department of Materials Science and Engineering,
IIT Kanpur, Kanpur 208016, India*

(Dated: June 3, 2019)

Abstract

Two dimensional magnetic materials, with tunable electronic properties could lead to new spintronic, magnetic and magneto-optic applications. Here, we explore intrinsic magnetic ordering in two dimensional monolayers of transition metal tri-halides (MX_3 , $\text{M} = \text{V}, \text{Cr}, \text{Mn}, \text{Fe}$ and Ni , and $\text{X} = \text{F}, \text{Cl}, \text{Br}$ and I), using density functional theory. We find that other than FeX_3 family which has an anti-ferromagnetic ground state, rest of the trihalides are ferromagnetic. Amongst these the VX_3 and NiX_3 family are found to have the highest magnetic transition temperature, beyond the room temperature. In terms of electronic properties, the tri-halides of Mn and Ni are either half metals or Dirac half metals, while the tri-halides of V , Fe and Cr are insulators. Among all the trihalides studied in this paper, we find the existence of very clean spin polarized Dirac half metallic state in MnF_3 , MnCl_3 , MnBr_3 , NiF_3 and NiCl_3 . These spin polarized Dirac half metals will be immensely useful for spin-current generation and other spintronic applications.

I. INTRODUCTION

Recent discovery of ferromagnetism in single layer CrI_3 and $\text{Cr}_2\text{Ge}_2\text{Te}_6$, has opened up the field of intrinsic magnetism in 2D materials to intense exploration.^{1,2} Magnetism in ultra-thin two dimensional (2D) materials opens up the exciting possibility of atomically thin and low dimensional magnetic storage, sensing, spintronic and optical devices.³⁻¹² Additionally, they can also be used to break time-reversal symmetry in 2D stacks for valley-tronics.⁴ Indeed, electrostatic gate control of magnetism in both CrI_3 and $\text{Cr}_2\text{Ge}_2\text{Te}_6$ has already been demonstrated,³⁻⁶ along with spin-filter device with giant tunnelling magnetoresistance.¹³⁻¹⁶ In addition to their applicability, 2D magnetism also opens the door to new quantum state of matter, existence of which was prohibited by the Mermin Wagner theorem.¹⁷

To understand the prohibition of spin-ordering in 2D systems by the Mermin Wagner theorem,¹⁷ let us have a look at the simplest model describing spin-spin interaction in a 2D system,

$$H = -J_{\parallel} \sum_{kl} (S_k^x S_{k+l}^x + S_k^y S_{k+l}^y) - J_{\perp} \sum_{kl} S_k^z S_{k+l}^z. \quad (1)$$

Here S_k^m denotes the $m = x, y, z$ component of the spin at site k , and the sum over k, l runs over the nearest neighbors. In Eq. (1), J_{\parallel} and J_{\perp} are the in-plane ($x - y$ plane) and out of plane spin exchange energy, respectively. If $J_{\perp} = 0$ and $J_{\parallel} \neq 0$, the Hamiltonian reduces to the X-Y Ising-spin model, and for $J_{\perp} = J_{\parallel} \neq 0$ the model reduces to the isotropic Heisenberg spin model. The Mermin Wagner theorem¹⁷ forbids finite temperature magnetic ordering in the isotropic X-Y, as well as the isotropic Heisenberg spin model (both classical and quantum) in one and two dimensions. This is a consequence of quantum and thermal fluctuations dominating over the spin-ordering phenomena. However, spontaneous magnetic ordering can still emerge in SU(2) symmetry broken cases such as the anisotropic Heisenberg model ($J_{\parallel} \neq J_{\perp}$), or the Ising model. In fact, Onsager demonstrated the theoretical possibility of a finite temperature magnetic transition in the two dimensional Ising model as early as 1944.¹⁸ The spin ordering observed using high-sensitivity microscopy (polar magneto-optical Kerr effect microscopy) technique in mono-layered CrI_3 is indeed found to be Ising like (below 45K).^{1,19,20} In case of $\text{Cr}_2\text{Ge}_2\text{Te}_6$, while no magnetic ordering is observed in the monolayer (at least till 4.7 K), the magnetic ordering in the bi-layer is described by the Heisenberg model with additional magnetic anisotropies^{2,19} (a term $\propto \sum_k (S_k^z)^2$).

Following CrI_3 and $\text{Cr}_2\text{Ge}_2\text{Te}_6$, 2D magnetism has also been experimentally reported

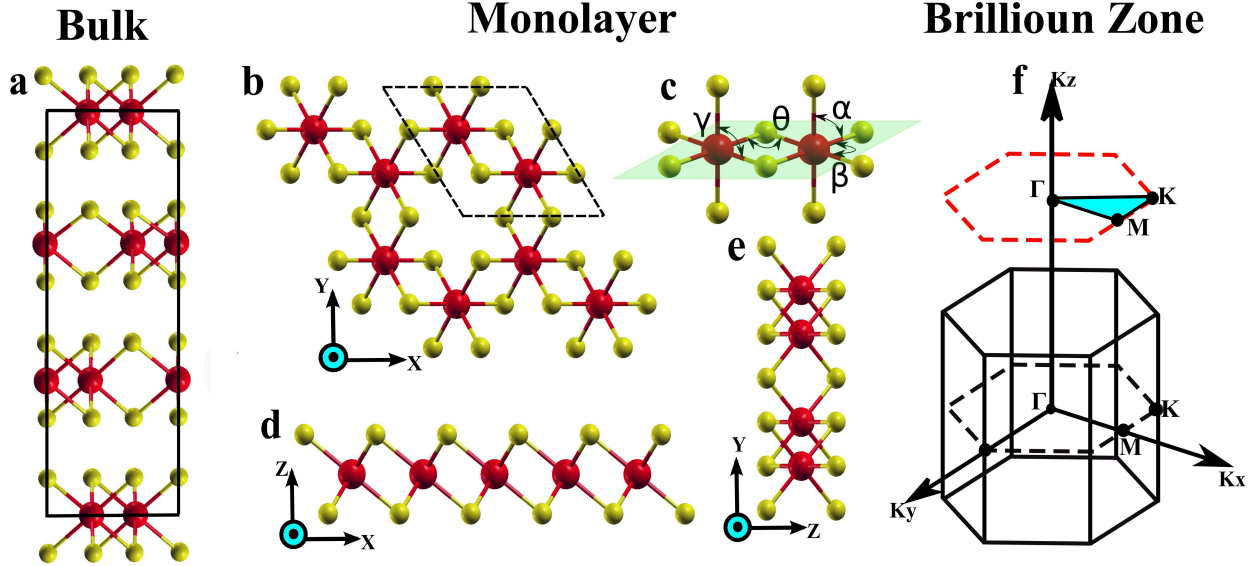


FIG. 1. Crystal structure and Brillouin zone of bulk and monolayer MX_3 . (a) BiI_3 type rhombohedral unit cell of bulk MX_3 . (b) Top view of monolayer MX_3 , with the hexagonal unit cell marked by the dashed line. (c) Six X atoms (yellow) forming an octahedron surrounding the M atom (red). (d) and (e) show different side views of MX_3 monolayers. (f) Brillouin zones of bulk (solid line) and monolayer (dashed line) MX_3 , corresponding to the unit cells shown in (a) and (b).

in FePS_3 ^{21,22} (Ising-type anti-ferromagnet) and MnSe_2 ²³ (ferromagnet), among others. In a more significant development, room temperature magnetism has been recently demonstrated in VSe_2 monolayers on van der Waals substrates.²⁴ Contrary to CrI_3 and $\text{Cr}_2\text{Ge}_2\text{Te}_6$, VSe_2 is paramagnetic in the bulk form. In addition to these, there have been theoretical predictions of magnetism in several other materials based on density functional theory and Monte-Carlo simulations.²⁵ These include several monolayers of easily exfoliable metal di-halides MX_2 ($\text{M} = \text{Fe}, \text{Co}, \text{Ni}, \text{Mn}, \text{V}$, and $\text{X} = \text{B}, \text{Cl}, \text{I}$),²⁶ and layered ternary compounds CrSiTe_3 , CrGeTe_3 and $\text{Cr}_2\text{Ge}_2\text{Te}_6$ of the telluride family.^{27,28} Several of the transition metal tri-halides such as CrX_3 ,^{29,30} OsCl_3 ,³¹ VCl_3 ,^{32,33} NiCl_3 ,³⁴ RuX_3 ,³⁵⁻³⁸ and MnX_3 ($\text{X} = \text{F}, \text{Cl}, \text{Br}, \text{I}$)³⁹ are also expected to have either a ferromagnetic or an anti-ferromagnetic ground state described by an Ising spin model.

Motivated by this recent interest in 2D magnetic materials, we present a comparative study of magnetism in different transition metal tri-halide monolayers. More specifically, we investigate the crystal structure, electronic and magnetic properties for 20 different MX_3

compounds (M= V, Cr, Mn, Fe and Ni, while X= F, Cl, Br, or I), using density functional theory. Not only we find several ferromagnetic 2D materials (V, Cr, Mn and Ni tri-halides), but also anti-ferromagnetic monolayers (Fe tri-halides), not reported so far in the literature. We also identify several spin polarized Dirac half-metals among the family of transition metal tri-halide monolayers. These have a large band-gap in one spin channel and a Dirac cone in the other, with Fermi velocities comparable to graphene. Such materials are ideal for making spintronic and other nano-electronic devices.

The paper is organized as follows: computational details are described in Sec. II. Results are presented along with detailed discussions in Sec. III. It contains a description of the crystal structure, analysis of binding energy in the context of stability of the monolayers and discussions on electronic and magnetic properties of transition metal tri-halide monolayers. Our findings are summarized in Sec. IV.

II. COMPUTATIONAL METHOD

Using density functional theory (DFT), we calculate the structural, electronic and magnetic properties of MX_3 monolayers. We use a plane-wave basis set with the cutoff energy of 80 Ry, and projector-augmented wave pseudo potentials, as implemented in the Quantum Espresso (QE) and VASP package.⁴⁰⁻⁴³ The electron-electron exchange correlation is treated within the framework of the generalized gradient approximation (GGA), as proposed by Perdrew-Burke-Ernzerhof (PBE).⁴⁴ Brillouin zone integrations are performed using a k -point grid of $32 \times 32 \times 1$. Perpendicular to the monolayers, a vacuum of 15 Å is applied to prevent the spurious interactions among replica images. All the structures are fully relaxed until the forces on each atom are less than 10^{-3} Ry/au and the energy difference between two successive ionic relaxation steps is less than 10^{-4} Ry. Note that, electronic band structure calculations based on GGA-PBE approximation yield consistent results in case of Quantum Espresso and VASP, while only the latter is used to perform more accurate hybrid functional (HSE06) based calculations.⁴⁵

III. RESULT AND DISCUSSION

A. Crystal Structure

Bulk transition metal tri-halides (MX_3) are known to exist in the form of layered materials bonded by weak van der Waals interactions. These materials are generally found either in monoclinic AlCl_3 or rhombohedral BiI_3 crystal structure.⁴⁶ A bulk unit cell of BiI_3 type is shown in Fig. 1(a), where monolayers are stacked in ABC sequence. Several of transition metal tri-halides are predicted to have low values of the cleavage energy, based on first principle calculations.^{20,29,30,47–49} Thus, in principle they can be exfoliated as atomically thin 2D materials from their bulk phases.

Recently, a single magnetic layer of CrI_3 has been successfully exfoliated from its bulk phase,¹ encouraging the exploration of monolayers of the tri-halide family of magnetic materials in 2D. In case of individual monolayers, the smallest repeat segment is a hexagonal unit cell, having two formula units of MX_3 in it [see Fig. 1(b)]. Each M atom is coordinated to six X atoms in an octahedral coordination, as shown in Fig. 1(c). Monolayers are not atomically flat and a layer of metal atoms are sandwiched between two layers of halide atoms, as shown in Fig. 1(d) and (e). The Brillouin zones (BZ) of the bulk (solid line) and monolayer (dashed line) MX_3 is illustrated in Fig. 1(f). The *ab-initio* optimized values of the lattice constants, bond lengths (M-X) and bond angles (M-X-M) of 20 different MX_3 structures (M = V, Cr, Mn, Fe and Ni, while X= F, Cl, Br, or I) are reported in Table I. We find that the fluorides have slightly higher value of θ (lying between $\sim 99^\circ - 104^\circ$) than that of chlorides, bromides and iodides (lying between $\sim 92^\circ - 94.5^\circ$). As expected, bond lengths and lattice constants depend on the size of the constituent atoms and increase with the size of the halogen atoms and our numbers are consistent with the values reported in the literature.^{33,34,39,50}

B. Binding Energy

Phonon dispersion calculations have already established the stability of several of the MX_3 monolayers.^{30,33,34,39} This strengthens the possibility of the existence of such a family of atomically thin and possibly magnetic 2D materials in free standing form. Some idea regarding the relative stability of the monolayer metal tri-halides can be obtained by

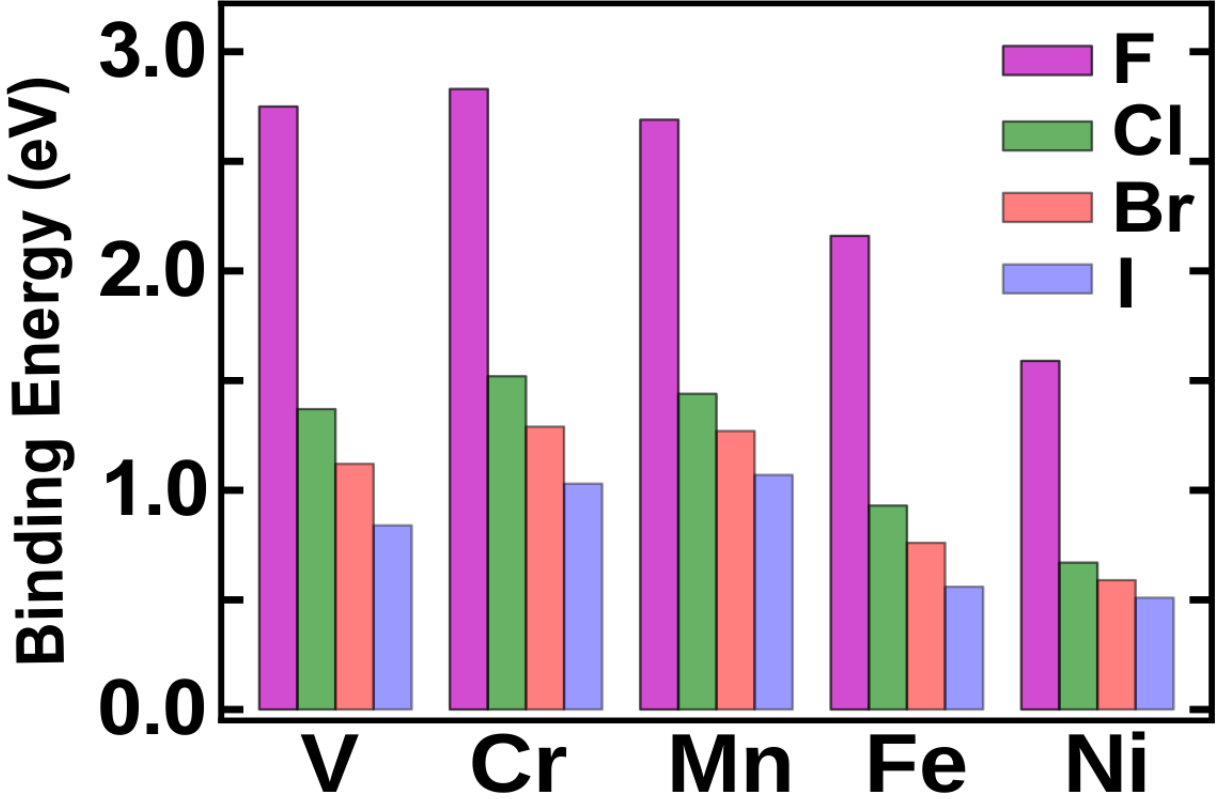


FIG. 2. A comparison of calculated binding energies of MX_3 monolayers. Irrespective of the transition metals, fluorides have the highest binding energy among the halides.

comparing their binding energies, defined as,^{51,52}

$$E_b = \frac{2E_M + 6E_X - E_{MX_3}}{8}, \quad (2)$$

where E_M , E_X , and E_{MX_3} are the total energies of the transition metal atom (M), halogen atom (X), and transition metal tri-halide monolayer (MX_3). According to our calculations, E_b of all the monolayers listed in Table I, are positive and lie in the range from 0.519 to 2.838 eV per atom. Note that, the binding energy for the cobalt tri-halide family are found to be negative (not shown in the table), indicating inherent instability of those structures and thus, they are not considered in this article. The calculated values of E_b listed in Table I are also shown in a bar graph for ease of comparison in Fig. 2. Evidently, the fluoride MX_3 's have the highest binding energies compared to other halides. We find that the E_b decreases with increasing size of the halogen atom. Also note that V, Cr and Mn tri-halides are likely to be more stable as compared to the Fe and Ni tri-halides.

Thus, our structural analysis predicts the exciting possibility of the existence of several

TABLE I. Calculated lattice constant ($a = b$), M-X bond length (d_{M-X}), bond angles, and binding energy (BE) of MX_3 monolayers. Different bond angles (α , β , γ and θ) are defined in Fig. 1(c).

MX_3	$a(\text{\AA})$	$d_{M-X}(\text{\AA})$	Bond-angle				BE (eV)
			α	β	γ	θ	
VF_3	5.34	1.95	95.5	75.8	95.0	104.0	2.756
VCl_3	5.97	2.39	93.1	87.9	89.5	92.0	1.370
VBr_3	6.33	2.54	92.7	87.8	89.7	92.1	1.127
VI_3	6.86	2.75	91.9	88.0	90.0	91.9	0.840
CrF_3	5.14	1.92	90.4	79.1	95.4	100	2.838
CrCl_3	5.97	2.35	93.1	85.8	90.6	94.0	1.520
CrBr_3	6.34	2.51	92.3	86.6	90.5	93.3	1.299
CrI_3	6.85	2.71	91.6	86.5	90.9	93.0	1.039
MnF_3	5.37	1.99	95.5	77.6	93.8	102.0	2.697
MnCl_3	6.10	2.40	94.9	85.8	89.8	94.0	1.445
MnBr_3	6.39	2.55	93.1	87.4	89.7	92.5	1.274
MnI_3	6.85	2.77	92.0	88.8	89.5	91.0	1.070
FeF_3	5.21	1.97	93.1	80.8	93.3	99.1	2.160
FeCl_3	6.02	2.40	93.3	87.4	89.7	92.5	0.931
FeBr_3	6.42	2.57	92.9	87.8	89.6	92.1	0.767
FeI_3	6.97	2.78	92.0	87.4	90.2	92.5	0.561
NiF_3	5.00	1.87	90.7	79.3	95.2	100.5	1.596
NiCl_3	5.82	2.29	93.0	85.8	90.6	94.5	0.679
NiBr_3	6.16	2.44	92.7	86.8	90.3	93.0	0.595
NiI_3	6.64	2.66	92.3	87.3	90.1	91.8	0.519

magnetic monolayers in the family of transition metal tri-halides, all having similar crystal structure. In fact the experimental discovery of 2D magnetic CrI_3 monolayers might just be the beginning of an exciting journey with magnetism in 2D transition metal tri-halides and other materials. Some of the transition metal tri-halides are already predicted to have magnetic ground state^{33,34,39,50}. In the next section, we do an exhaustive study of electronic and magnetic properties of all the 20 MX_3 monolayers listed in Table I.

TABLE II. Calculated value of exchange coupling constant (J), absolute magnetic moment per M atom (m_A), total magnetic moment per unit cell (m_T) and bandgap (E_g) for MX_3 monolayers.

MX_3	J (meV)	m_A (μ_B)	m_T (μ_B)	E_g (eV)
VF_3	32.25	1.89	4	3.23
VCl_3	21.60	1.96	4	2.51
VBr_3	18.43	2.03	4	2.12
VI_3	17.78	2.17	4	1.26
CrF_3	0.96	2.86	6	5.09
$CrCl_3$	0.85	2.93	6	3.84
$CrBr_3$	2.57	3.03	6	2.87
CrI_3	1.70	3.15	6	1.85
MnF_3	8.47	3.87	8	0
$MnCl_3$	1.62	3.95	8	0
$MnBr_3$	1.76	4.02	8	0
MnI_3	1.90	4.05	8	0
FeF_3	-2.57	4.15	0	5.10
$FeCl_3$	-1.68	4.02	0	3.03
$FeBr_3$	-2.33	3.94	0	2.57
FeI_3	-1.47	3.82	0	1.83
NiF_3	76.7	0.86	2	0
$NiCl_3$	43.9	0.94	2	0
$NiBr_3$	51.3	1.02	2	0
NiI_3	46.7	1.09	2	0

C. Electronic and Magnetic Ground States

Using the optimized crystal structures (see Table I for details), the electronic band structures of MX_3 monolayers are calculated and all of the 20 monolayers are found to have a magnetic ground state. In all MX_3 with $M = V, Cr, Mn$ and Ni , the ferromagnetic ground state is obtained, while in case of Fe the anti-ferromagnetic ground state is preferred.

The HSE06 based electronic band structure and the spin projected density of states of one

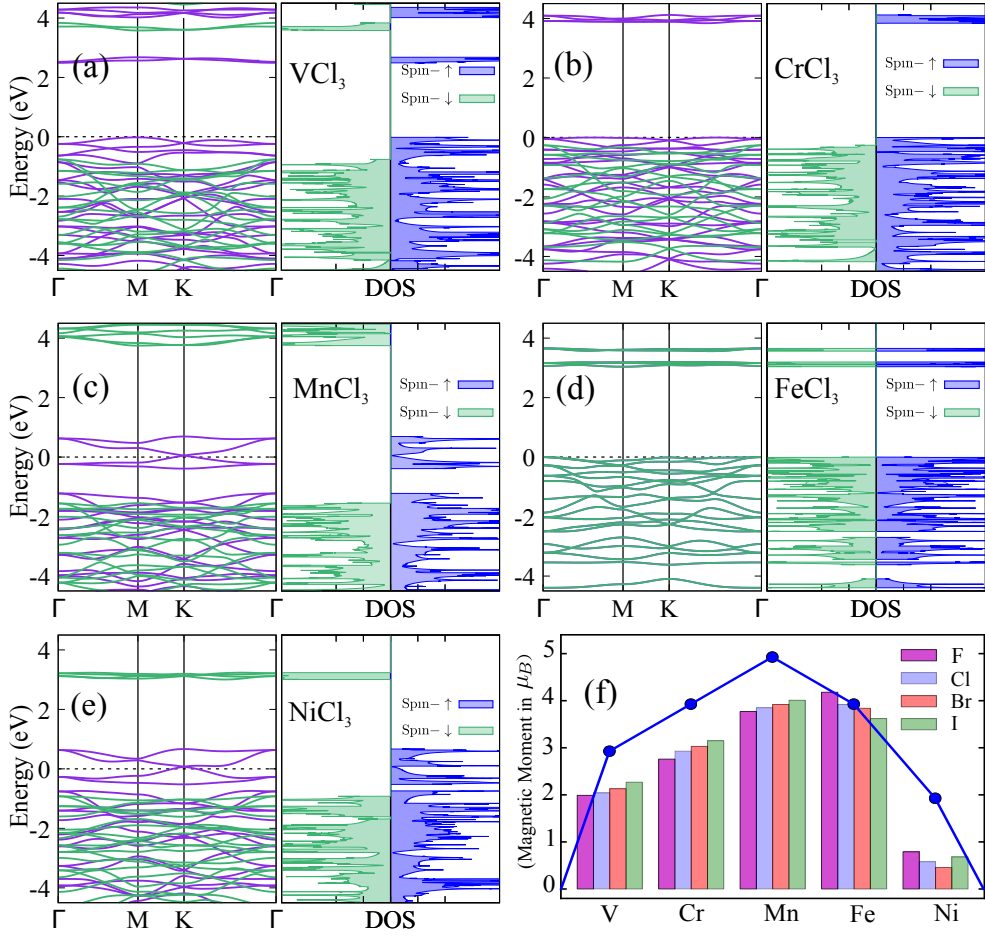


FIG. 3. Spin polarized electronic band structure (using HSE06) along the lines joining the high symmetry points in the first Brillouin zone and spin projected density of states (DOS) for monolayer of (a) VCl₃, (b) CrCl₃, (c) MnCl₃, (d) FeCl₃, (e) NiCl₃ in their magnetic ground state. (f) Magnetic moments of M-atoms in MX₃ monolayer.

representative tri-halide (chosen to be tri-chloride) in its magnetic ground state is shown in Fig. 3(a)-(e) and their magnetic moments are compared in Fig. 3(f). For a complete picture, please refer to the Supplementary Information (SI), where a comparison between the PBE and HSE06 based electronic band-structure and spin projected density of states are presented for all the tri-halides studied in this paper. Both the functionals predict qualitatively similar band-structures with bandgap underestimated by PBE, as expected, in case of all the MX₃ monolayer families, except for monolayer VX₃. This is discussed in detail below.

We find that the electronic and magnetic ground states of all the tri-halides belonging

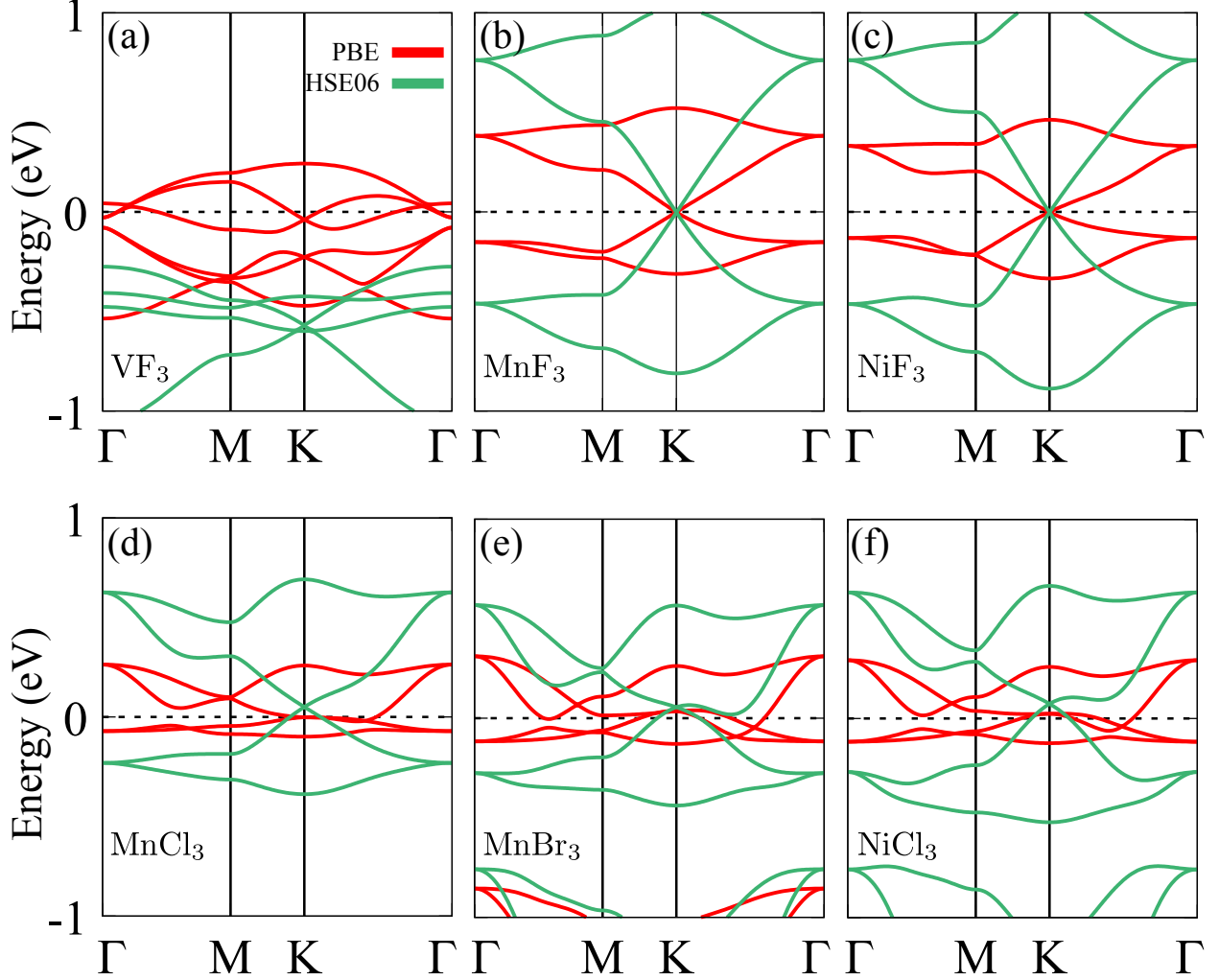


FIG. 4. The spin polarized Dirac half metallic band structure along the high symmetry directions (Γ -K-M- Γ) for (a) VF_3 and (b) MnF_3 , (c) NiF_3 , (d) MnCl_3 , (e) MnBr_3 and (f) NiCl_3 . Only the \uparrow -spin bands are shown for clarity. The \downarrow -spin bands are gapped, as shown in Fig. 3, making all of them Dirac half metals. The Fermi level is shown with black dashed line and is set at 0 eV.

to a particular family of transition metal are similar [see Table II]. Our calculations reveal that tri-halides based on Mn and Ni have a ferromagnetic ground state with either metallic or semi-metallic character with a spin polarized Dirac cone. As shown in Fig. 3 (c) and (e), MnCl_3 and NiCl_3 have very clean spin polarized doubly degenerate Dirac node at the Fermi energy, with two linearly dispersing \uparrow -spin bands crossing each other. They also have relatively low density (linearly vanishing) of states at the Fermi level because of the linearly dispersing (Dirac like) bands in vicinity of the K -point. Similar behavior is observed in case of several other members of the family, except for tri-iodides, which clearly show a metallic

band-structure, with Fermi level (E_F) crossing the electronic bands at several points in the Brillouin zone, resulting in a relatively larger density of states at the E_F (see SI). The \downarrow -spin bands in case of each of the Mn and Ni tri-halides are similar to that of insulators, with a surprisingly large energy gap of more than 2 eV (see SI). Hence, tri-halides belonging to the Mn and Ni family can be categorized as Dirac half-metals or half-semimetals (based on the character of the \uparrow -spin band), as the \downarrow -spin states are always gapped.

Similar to Mn and Ni family, the tri-halides based on V are also ferromagnetic. However, they are found to have either a spin polarized Dirac semimetal or metal like state in PBE calculations (similar to Ref. [33]), as opposed to insulating character in HSE06 calculations (band gap ranging from 1.26 eV to 3.23 eV, see Table II). The HSE06 based band structure of VCl_3 is shown in Fig. 3 (a), which is clearly different from the gap-less energy spectrum obtained from PBE as well as strongly constrained and appropriately normed (SCAN)⁵³ based calculations (see SI). The hybrid functional calculations push all the up-spin bands lower in energy into the valance band, as opposed to PBE or SCAN calculations. This behavior is observed in case of all the tri-halides belonging to the V family (see SI). Particularly in case of VF_3 , PBE and SCAN calculations predict a spin-polarized linearly dispersing band (in vicinity of the K -point) while a large bandgap is observed in the HSE06 calculation. Since the HSE06 calculations differ markedly from PBE, SCAN and PBE + U based results,³³ we believe that the HSE06 functional is not well suited for exploring metallic magnetic states in V based compounds. However, it is not very clear why does the difference appear only in case of V, while other transition metals studied here show qualitatively consistent results (see SI for details).

The most remarkable feature observed so far is the existence of several Mn, Ni and V (possibly) tri-halide monolayers, with fully spin polarized bands having very clean 2D massless Dirac like dispersion, similar to that of graphene. In hindsight, the existence of 2D Dirac cone in these materials is not unexpected, as the transition metal atoms form a honeycomb lattice by themselves, similar to the arrangement of carbon atoms in graphene. Some of these Dirac half metals are shown in Fig. 4 (a)-(f). In particular MnF_3 , MnCl_3 , MnBr_3 , NiF_3 , and NiCl_3 show very clean Dirac half metal state in both PBE as well as HSE06 calculations. These spin polarized Dirac half metals are very interesting from a fundamental physics point of view, as well as for use in spin current generation and other spintronic applications.^{54,55}

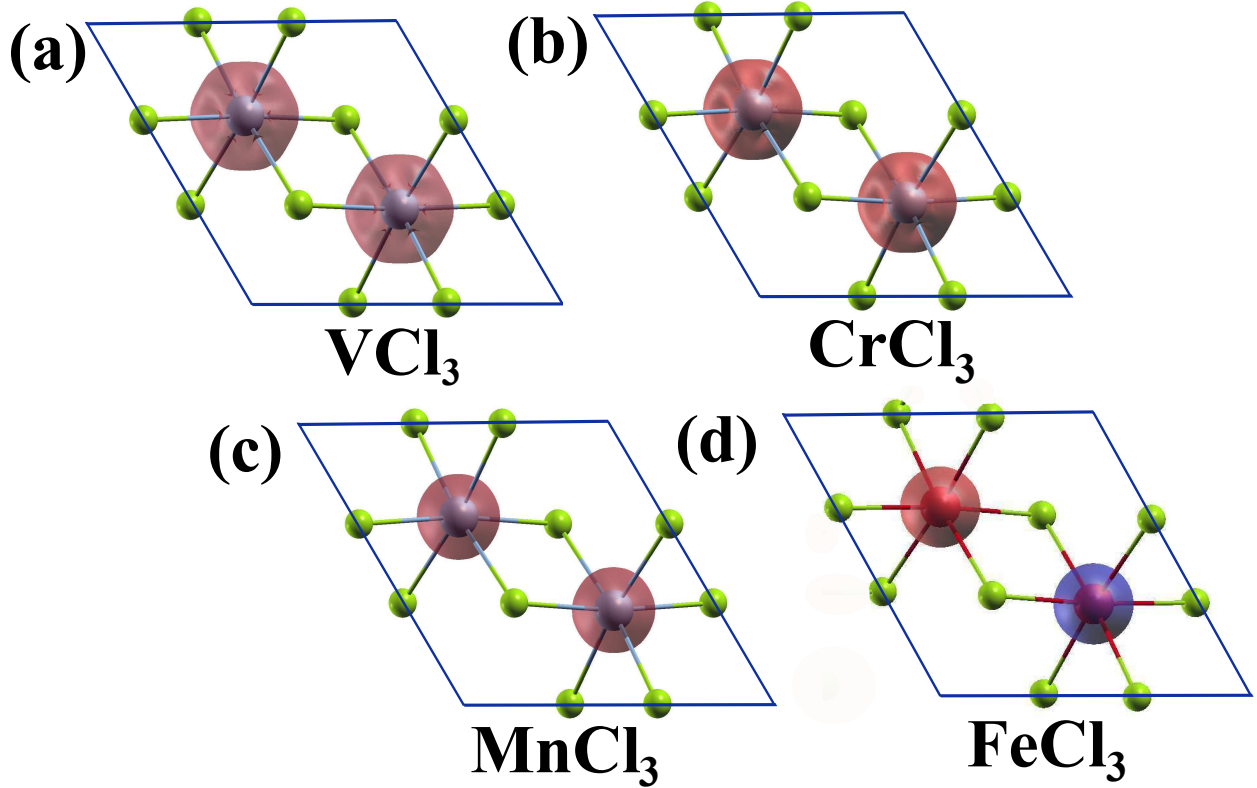


FIG. 5. Spin-polarized charge densities for (a) VCl_3 , (b) CrCl_3 , (c) MnCl_3 , and (d) FeCl_3 monolayer in their ground state. Red denotes the up-spin while blue denotes the down spin in the 3d orbital of the transition metal in MX_3 monolayers. Evidently only FeCl_3 is anti-ferromagnetic while all the others are ferromagnetic.

Unlike half metallic or half semi-metallic tri-halides of Mn and Ni, Cr based tri-halides are found to be insulating (band gap ranging from 1.85 eV to 5.09 eV, see Table II), with a ferromagnetic ground state. This is consistent with the experimental observation of ferromagnetic ground state in CrI_3 . Electronic band structure of CrCl_3 is shown in Fig. 3(b) and qualitatively similar trends are observed for other members of the Cr family (shown explicitly in SI). Note that, magnitude of band gap in case of \uparrow and \downarrow spin state is different for all the Cr tri-halides.

Similar to Cr, Fe-based tri-halides are also insulating (band gap ranging from 1.83 eV to 5.10 eV, see Table II). Interestingly, this is the only family with an antiferromagnetic ground state. Electronic band structure of FeCl_3 is shown in Fig. 3(d), which is qualitatively similar for other members of the FeX_3 monolayers family as well(see SI). In general, for insulating transition metal tri-halides, magnitude of the bandgap decreases with the size of the halogen

atom and nearly 50% reduction is observed between the two extremes, occupied by the fluoride and iodide, respectively (see Table II).

Having discussed the band structure, we now analyze the magnetic properties of the transition metal tri-halides. The calculated values of magnetic moment per transition metal atom for all the MX_3 monolayers studied in this paper are illustrated in Fig. 3(f). Since the transition metal ions are octahedrally coordinated to the halogen atoms, they can exist in either high or low spin state due to crystal field splitting. High crystal field splitting leads to low spin state and vice versa. Based on calculated values of magnetic moment [see Table II and Fig. 3(f)], Mn^{3+} ($\approx 4\mu_B$) is found to exist in high spin state, while low spin state is observed in case of Ni^{3+} ($\approx 1\mu_B$). Surprisingly, magnetic moment of iron is found to be $\approx 4\mu_B$, which is neither high spin ($5\mu_B$), nor low spin ($1\mu_B$) state of Fe^{3+} . Similar results have been found in a recently published study, which also takes into account the effect of strain, as well as Hubbard- U .⁵⁶ Magnetic moment of vanadium and chromium is found to be consistent with their respective values in the +3 oxidation state, which is equal to $2\mu_B$ and $3\mu_B$ for V^{3+} and Cr^{3+} , respectively. We find that for V, Mn, Cr and Ni based tri-halides the magnetic moment increases marginally with the size of the halogen atom, while in Fe, it decreases slightly from F to I.

Details of the calculated magnetic properties are reported in Table II. The ferromagnetic and antiferromagnetic ground states can be identified by non-zero and zero total magnetic moment (m_T) per unit cell, respectively. A comparison of absolute magnetic moment (m_A) per M atom with m_T [reported in Table II, and shown in Fig. 3(f)] elucidates that the magnetism of MX_3 monolayers originates primarily from the transition metal atoms. However, a small ferromagnetic (antiferromagnetic) coupling is observed between the halogen and metal atom in case of fluorides and chlorides (bromides and iodides). The role of the $3d$ transition metal orbitals in the magnetism in MX_3 monolayers is further emphasized by plotting the spin densities of V, Cr, Mn and Fe tri-chlorides in Fig. 5 (a)-(d). As discussed previously, only the Fe tri-halides have an anti-ferromagnetic ground state, with magnetic moments of the two Fe atoms in the unit cell pointed in the opposite directions. This is shown for FeCl_3 in Fig. 5(d).

A crude estimate of the exchange coupling and the transition temperature of the magnetic ground state can be obtained by modelling the system as a spin- S quantum Ising model on

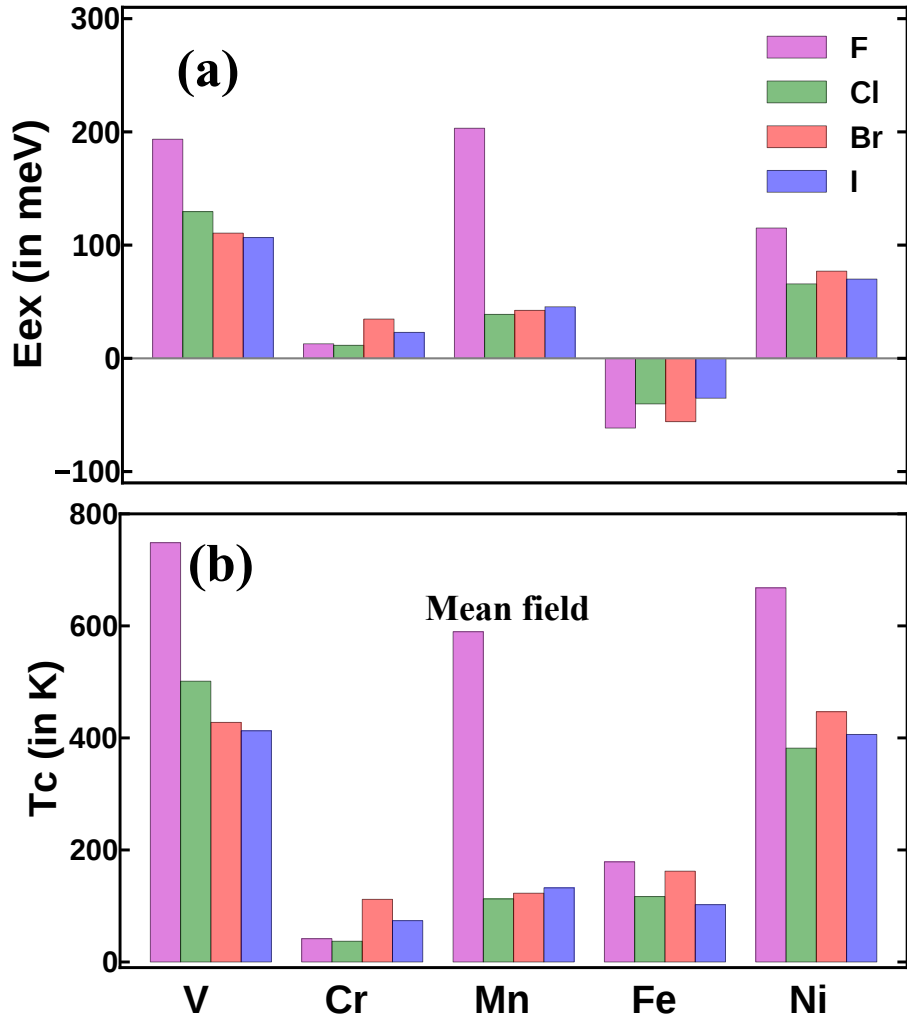


FIG. 6. (a) A comparison of exchange energies of all the metal tri-halides studied in this paper. While Fe constitutes a family of anti-ferromagnetic tri-halides with negative E_{ex} , rest of the transition metal tri-halides are ferromagnetic with positive E_{ex} . (b) The corresponding mean field Curie-Weiss transition temperature calculated using the spin- S quantum Ising model.

the honeycomb lattice. The spin- S Ising model can be expressed as,

$$H = - \sum_{\langle ij \rangle} J_{ij} S_i^z S_j^z . \quad (3)$$

Here, J_{ij} is the exchange coupling constant between sites i and j sites hosting the magnetic moment of the hybridized transition metal with $S_{i/j}^z = m_A/2$. The value of S^z is taken to be equal to 1, 3/2, 2, 2 and 1/2 for $M = \text{V, Cr, Mn, Fe, and Ni}$ series, respectively (see Table II and Fig. 3(f)). As discussed in the previous paragraph, we find a relatively weak

ferromagnetic or anti-ferromagnetic M-X coupling, compared to the much stronger coupling between the two neighboring M atoms. Thus, for simplicity we ignore the M-X coupling, and consider only an isotropic nearest neighbor (in M-M) Ising Hamiltonian in Eq. 3.

In an isotropic model with nearest neighbor interactions, $J_{ij} = J$ and the sign of J dictates the magnetic ordering in the crystal. Positive value of J leads to ferromagnetic ordering and negative value of J results in anti-ferromagnetic configuration. Using the isotropic spin- S Ising model with nearest neighbor interactions, J is given by^{34,57}

$$J = \frac{E_{\text{ex}}}{2z_0(S^z)^2}. \quad (4)$$

Here $z_0 = 3$ is the co-ordination number of the M-atoms forming a honeycomb lattice. The exchange energy in Eq. 4 is defined as the half of the of the energy difference between the anti-ferromagnetic and ferromagnetic state.⁵⁷ Calculated values of E_{ex} for all the MX_3 monolayers are compared in Fig. 6(a). We find that fluorides have higher value of exchange energy than rest of the trihalides, Cr-family being the only exception. In general, the V based tri-halide family have reasonably large value of E_{ex} , followed by Ni, Mn, Fe and Cr tri-halides.

The magnetic transition temperature (T_c) can be estimated using the Curie-Weiss mean field theory for a quantum spin- S Ising model. For $T > T_c$, the ordered magnetic state is completely destroyed by thermal energy, yielding a paramagnetic (non-magnetic) state with random spin orientation and zero net magnetic moment in the absence of an external magnetic field. Within the mean field theory, the transition temperature is given by⁵⁸

$$T_c = \frac{z_0 J S^z (S^z + 1)}{3k_B}, \quad (5)$$

where k_B denotes the Boltzmann constant. Calculated values are illustrated in Fig. 6(b). As shown in the figure, the VX_3 and the NiX_3 families have relatively higher transition temperatures, ranging from 400 to 800 K. In case of MnX_3 and FeX_3 families, T_c lies in the range of 100 to 200 K (other than MnF_3 , having a $T_c \sim 600$ K). Other than the bromide, members belonging to the CrX_3 family have sub 100 K T_c values, which are lower than rest of the trihalide families. Note that, the mean-field theory is known to over-estimate the T_c . For example, while experimentally observed T_c value of CrI_3 is reported to be 45 K,¹ our calculations predict it to be 75 K. However, the relative trend between the T_c of different materials should more or less be along the lines of Fig. 6(b).

IV. CONCLUSION

Motivated by the recent discovery of two dimensional magnetic materials, we do a comparative study of several transition metal tri-halide monolayers based on *ab-initio* calculations. We find that the tri-halides of V, Mn, and Ni are either metallic or semimetallic with primarily a ferromagnetic ground state. Cr based tri-halides are insulators with a ferromagnetic ground state. Fe based tri-halides are anti-ferromagnetic insulators. We also predict VX_3 and NiX_3 family of tri-halides to have relatively high magnetic transition temperature. The transition metal tri-halides, MnF_3 , $MnCl_3$, $MnBr_3$, NiF_3 , $NiCl_3$ and VF_3 are found to host very clean spin polarized Dirac half metallic states. These spin polarized Dirac half metals are very useful for spintronic applications and devices. Amongst these, VF_3 , $NiCl_3$ and MnF_3 monolayers may even be in thermodynamically stable ferro-magnetic state at room temperature.

V. ACKNOWLEDGMENTS

The authors acknowledge funding from the Ramanujan fellowship research grant, the DST Nanomission project and SERB (EMR/2017/004970). The authors also thank the computer center of IIT Kanpur for providing HPC facility.

* amitag@iitk.ac.in

† bsomnath@iitk.ac.in

¹ B. Huang, G. Clark, E. Navarro-Moratalla, D. R. Klein, R. Cheng, K. L. Seyler, D. Zhong, E. Schmidgall, M. A. McGuire, D.H. Cobden, H. David, W. Yao, D. Xiao, P. Jarillo-Herrero, and X. Xu, "Layer-dependent ferromagnetism in a Van der Waals crystal down to the monolayer limit," *Nature* **546**, 270 (2017)

² Cheng Gong, Lin Li, Zhenglu Li, Huiwen Ji nad Alex Stern, Yang Xia, Ting Cao, Wei Bao, Chenzhe Wang, Yuan Wang, Z. Q. Qiu, R. J. Cava, Steven G. Louie, Jing Xia, and Xiang Zhang, "Discovery of intrinsic ferromagnetism in two-dimensional van der waals crystals," *Nature* **546**, 265

- ³ Bevin Huang, Genevieve Clark, Dahlia R. Klein, David MacNeill, Efrén Navarro-Moratalla, Kyle L. Seyler, Nathan Wilson, Michael A. McGuire, David H. Cobden, Di Xiao, Wang Yao, Pablo Jarillo-Herrero, and Xiaodong Xu, “Electrical control of 2D magnetism in bilayer CrI₃,” [Nat. Nanotechnol. **13**, 1–5 \(2018\)](#)
- ⁴ Shengwei Jiang, Lizhong Li, Zefang Wang, Kin Fai Mak, and Jie Shan, “Controlling magnetism in 2D CrI₃ by electrostatic doping,” [Nat. Nanotechnol. , 1–5 \(2018\)](#)
- ⁵ Kenneth S. Burch, “Electric switching of magnetism in 2D,” [Nat. Nanotechnol. **13**, 1 \(2018\)](#)
- ⁶ Wenyu Xing, Yangyang Chen, Patrick M Odenthal, Xiao Zhang, Wei Yuan, Tang Su, Qi Song, Tianyu Wang, Jiangnan Zhong, Shuang Jia, X C Xie, Yan Li, and Wei Han, “Electric field effect in multilayer Cr₂Ge₂Te₆: a ferromagnetic 2d material,” [2D Materials **4**, 024009 \(2017\)](#)
- ⁷ Kyle L. Seyler, Ding Zhong, Dahlia R. Klein, Shiyuan Gao, Xiaou Zhang, Bevin Huang, Efrén Navarro-Moratalla, Li Yang, David H. Cobden, Michael A. McGuire, Wang Yao, Di Xiao, Pablo Jarillo-Herrero, and Xiaodong Xu, “Ligand-field helical luminescence in a 2D ferromagnetic insulator,” [Nat. Phys. **14**, 277–281 \(2018\)](#)
- ⁸ Mohsen Yarmohammadi and Bui Dinh Hoi, “A controllable magneto-topological property and band gap engineering in 2d ferromagnetic Lieb lattice,” [Journal of Magnetism and Magnetic Materials **464**, 103 – 107 \(2018\)](#)
- ⁹ P.A. Igoshev, A.V. Zarubin, A.A. Katanin, and V.Yu. Irkhin, “Ferromagnetism, spiral magnetic structures and phase separation in the two-dimensional Hubbard model,” [Journal of Magnetism and Magnetic Materials **324**, 3601 – 3604 \(2012\)](#)
- ¹⁰ Yuliang Mao, Haiqiao Xu, Jianmei Yuan, and Jianxin Zhong, “Functionalization of the electronic and magnetic properties of silicene by halogen atoms unilateral adsorption: a first-principles study,” [Journal of Physics: Condensed Matter **30**, 365001 \(2018\)](#)
- ¹¹ Nan Gao, Wei Tao Zheng, and Qing Jiang, “Density functional theory calculations for two-dimensional silicene with halogen functionalization,” [Phys. Chem. Chem. Phys. **14**, 257–261 \(2012\)](#)
- ¹² Minglei Sun, Sake Wang, Jin Yu, and Wencheng Tang, “Hydrogenated and halogenated blue phosphorene as Dirac materials: A first principles study,” [Applied Surface Science **392**, 46 – 50 \(2017\)](#)
- ¹³ Tiancheng Song, Xinghan Cai, Matisse Wei-Yuan Tu, Xiaou Zhang, Bevin Huang, Nathan P Wilson, Kyle L Seyler, Lin Zhu, Takashi Taniguchi, Kenji Watanabe, Michael A McGuire,

- David H Cobden, Di Xiao, Wang Yao, and Xiaodong Xu, “Giant tunneling magnetoresistance in spin-filter van der Waals heterostructures,” *Science* (80-.). **4851**, eaar4851 (2018)
- ¹⁴ D. R. Klein, D. MacNeill, J. L. Lado, D. Soriano, E. Navarro-Moratalla, K. Watanabe, T. Taniguchi, S. Manni, P. Canfield, J. Fernández-Rossier, and P. Jarillo-Herrero, “Probing magnetism in 2D van der Waals crystalline insulators via electron tunneling,” *Science* (80-.). **1222**, 1–9 (2018)
- ¹⁵ Hyun Ho Kim, Bowen Yang, Tarun Patel, Francois Sfigakis, Chenghe Li, Shangjie Tian, Hechang Lei, and Adam W. Tsen, “One million percent tunnel magnetoresistance in a magnetic van der waals heterostructure,” *Nano Letters* **18**, 4885–4890 (2018)
- ¹⁶ Zhe Wang, Ignacio Gutiérrez-Lezama, Nicolas Ubrig, Martin Kroner, Marco Gibertini, Takashi Taniguchi, Kenji Watanabe, Ataç Imamoğlu, Enrico Giannini, and Alberto F. Morpurgo, “Very large tunneling magnetoresistance in layered magnetic semiconductor CrI_3 ,” *Nature Communications* **9**, 2516 (2018)
- ¹⁷ N. D. Mermin and H. Wagner, “Absence of Ferromagnetism or Antiferromagnetism in One- or Two-Dimensional Isotropic Heisenberg Models,” *Phys. Rev. Lett.* **17**, 1133–1136 (1966)
- ¹⁸ Lars Onsager, “Crystal statistics. I. A two-dimensional model with an order-disorder transition,” *Phys. Rev.* **65**, 117–149 (1944)
- ¹⁹ Nitin Samarth, “Condensed-matter physics: Magnetism in flatland,” *Nature* **546**, 216–218 (2017)
- ²⁰ Michael A. McGuire, Hemant Dixit, Valentino R. Cooper, and Brian C. Sales, “Coupling of crystal structure and magnetism in the layered, ferromagnetic insulator CrI_3 ,” *Chemistry of Materials* **27**, 612–620 (2015)
- ²¹ Xingzhi Wang, Kezhao Du, Yu Yang Fredrik Liu, Peng Hu, Jun Zhang, Qing Zhang, Man Hon Samuel Owen, Xin Lu, Chee Kwan Gan, Pinaki Sengupta, Christian Kloc, and Qihua Xiong, “Raman spectroscopy of atomically thin two-dimensional magnetic iron phosphorus trisulfide (FePS_3) crystals,” *2D Materials* **3**, 031009 (2016)
- ²² Jae Ung Lee, Sungmin Lee, Ji Hoon Ryoo, Soonmin Kang, Tae Yun Kim, Pilkwang Kim, Cheol Hwan Park, Je Geun Park, and Hyeonsik Cheong, “Ising-Type Magnetic Ordering in Atomically Thin FePS_3 ,” *Nano Lett.* **16**, 7433–7438 (2016)
- ²³ Dante J. O’Hara, Tiancong Zhu, Amanda H. Trout, Adam S. Ahmed, Yunqiu Kelly Luo, Choong Hee Lee, Mark R. Brenner, Siddharth Rajan, Jay A. Gupta, David W. McComb, and

- Roland K. Kawakami, “Room Temperature Intrinsic Ferromagnetism in Epitaxial Manganese Selenide Films in the Monolayer Limit,” *Nano Lett.* **18**, 3125–3131 (2018)
- ²⁴ Manuel Bonilla, Sadhu Kolekar, Yujing Ma, Horacio Coy Diaz, Vijaysankar Kalappattil, Raja Das, Tatiana Eggers, Humberto R. Gutierrez, Manh-Huong Phan, and Matthias Batzill, “Strong room-temperature ferromagnetism in VSe₂ monolayers on van der Waals substrates,” *Nat. Nanotechnol.* **13**, 289–294 (2018)
- ²⁵ Yu Zhu, Xianghua Kong, Trevor David Rhone, and Hong Guo, “Systematic search for two-dimensional ferromagnetic materials,” *Phys. Rev. Materials* **2**, 081001 (2018)
- ²⁶ Vadym V. Kulish and Wei Huang, “Single-layer metal halides mx₂ (x = cl, br, i): stability and tunable magnetism from first principles and monte carlo simulations,” *J. Mater. Chem. C* **5**, 8734–8741 (2017)
- ²⁷ Xingxing Li and Jinlong Yang, “Cr_xte₃ (x = si, ge) nanosheets: two dimensional intrinsic ferromagnetic semiconductors,” *J. Mater. Chem. C* **2**, 7071–7076 (2014)
- ²⁸ Shenghang Wu, Lihai Wang, Bin Gao, Yazhong Wang, Yoon Soek Oh, Sang-Wook Cheong, Jiawang Hong, and Xueyun Wang, “The direct observation of ferromagnetic domain of single crystal crsite₃,” *AIP Advances* **8**, 055016 (2018)
- ²⁹ Junyi Liu, Qiang Sun, Yoshiyuki Kawazoe, and Puru Jena, “Exfoliating biocompatible ferromagnetic cr-trihalide monolayers,” *Phys. Chem. Chem. Phys.* **18**, 8777–8784 (2016)
- ³⁰ Wei-Bing Zhang, Qian Qu, Peng Zhu, and Chi-Hang Lam, “Robust intrinsic ferromagnetism and half semiconductivity in stable two-dimensional single-layer chromium trihalides,” *J. Mater. Chem. C* **3**, 12457–12468 (2015)
- ³¹ Xian-Lei Sheng and Branislav K. Nikolić, “Monolayer of the 5d transition metal trichloride oscl₃: A playground for two-dimensional magnetism, room-temperature quantum anomalous hall effect, and topological phase transitions,” *Phys. Rev. B* **95**, 201402 (2017)
- ³² Yungang Zhou, Haifeng Lu, Xiaotao Zu, and Fei Gao, “Evidencing the existence of exciting half-metallicity in two-dimensional ticl₃ and vcl₃ sheets,” *Scientific Reports* **6**, 19407 (2016)
- ³³ Junjie He, Shuangying Ma, Pengbo Lyu, and Petr Nachtigall, “Unusual dirac half-metallicity with intrinsic ferromagnetism in vanadium trihalide monolayers,” *J. Mater. Chem. C* **4**, 2518–2526 (2016)
- ³⁴ Junjie He, Xiao Li, Pengbo Lyu, and Petr Nachtigall, “Near-room-temperature chern insulator and dirac spin-gapless semiconductor: nickel chloride monolayer,” *Nanoscale* **9**, 2246–2252

- (2017)
- ³⁵ S. Sarikurt, Y. Kadioglu, F. Ersan, E. Vatansever, O. Akturk, Y. Yuksel, U. Akinci, and E. Akturk, “Electronic and magnetic properties of monolayer -rucl_3 : a first-principles and monte carlo study,” *Phys. Chem. Chem. Phys.* **20**, 997–1004 (2018)
- ³⁶ F. Iyikanat, M. Yagmurcukardes, R. T. Senger, and H. Sahin, “Tuning electronic and magnetic properties of monolayer [small alpha]- rucl_3 by in-plane strain,” *J. Mater. Chem. C* **6**, 2019–2025 (2018)
- ³⁷ Daniel Weber, Leslie M. Schoop, Viola Duppel, Judith M. Lippmann, Jrgen Nuss, and Bettina V. Lotsch, “Magnetic properties of restacked 2d spin 1/2 honeycomb rucl_3 nanosheets,” *Nano Letters* **16**, 3578–3584 (2016), pMID: 27176463
- ³⁸ Fatih Ersan, Erol Vatansever, Sevil Sarikurt, Yusuf Yksel, Yelda Kadioglu, H. Duygu Ozaydin, Olcay zengi Aktrk, mit Aknc, and Ethem Aktrk, “Exploring the electronic and magnetic properties of new metal halides from bulk to two-dimensional monolayer: Rux_3 ($x=\text{br}, \text{i}$),” *Journal of Magnetism and Magnetic Materials* **476**, 111 – 119 (2019)
- ³⁹ Qilong Sun and Nicholas Kioussis, “Prediction of manganese trihalides as two-dimensional dirac half-metals,” *Phys. Rev. B* **97**, 094408 (2018)
- ⁴⁰ P. Giannozzi and et al., “Quantum espresso: A modular and open-source software project for quantum simulations of materials,” *J. Phys. Condens. Matter* **21**, 395502 (2009)
- ⁴¹ P. E. Blöchl, “Projector augmented-wave method,” *Phys. Rev. B* **50**, 17953–17979 (1994)
- ⁴² G. Kresse and D. Joubert, “From ultrasoft pseudopotentials to the projector augmented-wave method,” *Phys. Rev. B* **59**, 1758–1775 (1999)
- ⁴³ G. Kresse and J. Furthmüller, “Efficient iterative schemes for ab initio total-energy calculations using a plane-wave basis set,” *Phys. Rev. B* **54**, 11169–11186 (1996)
- ⁴⁴ J. P. Perdew, K. Burke, and M. Ernzerhof, “Generalized Gradient Approximation Made Simple,” *Phys. Rev. Lett.* **77**, 3865–3868 (1996)
- ⁴⁵ Jochen Heyd, Gustavo E. Scuseria, and Matthias Ernzerhof, “Hybrid functionals based on a screened coulomb potential,” *The Journal of Chemical Physics* **118**, 8207–8215 (2003)
- ⁴⁶ Michael A. McGuire, “Crystal and magnetic structures in layered, transition metal dihalides and trihalides,” *Crystals* **7** (2017), 10.3390/cryst7050121
- ⁴⁷ Hongbo Wang, Fengren Fan, Shasha Zhu, and Hua Wu, “Doping enhanced ferromagnetism and induced half-metallicity in cri_3 monolayer,” *EPL (Europhysics Letters)* **114**, 47001 (2016)

- ⁴⁸ H Wang, V Eyert, and U Schwingenschlgl, “Electronic structure and magnetic ordering of the semiconducting chromium trihalides CrI_3 , CrBr_3 , and CrI_3 ,” [Journal of Physics: Condensed Matter](#) **23**, 116003 (2011)
- ⁴⁹ J L Lado and J Fernandez-Rossier, “On the origin of magnetic anisotropy in two dimensional CrI_3 ,” [2D Materials](#) **4**, 035002 (2017)
- ⁵⁰ Sheng-shi Li, Ya-ping Wang, Shu-jun Hu, Duo Chen, Chang-wen Zhang, and Shi-shen Yan, “Robust half-metallicity in transition metal tribromide nanowires,” [Nanoscale](#) **10**, 15545–15552 (2018)
- ⁵¹ Pan Liu, Feng Lu, Maokun Wu, Xiaoguang Luo, Yahui Cheng, Xue-Wei Wang, Weichao Wang, Wei-Hua Wang, Hui Liu, and Kyeongjae Cho, “Electronic structures and band alignments of monolayer metal trihalide semiconductors MX_3 ,” [J. Mater. Chem. C](#) **5**, 9066–9071 (2017)
- ⁵² Fengxian Ma, Mei Zhou, Yalong Jiao, Guoping Gao, Yuantong Gu, Ante Bilic, Zhongfang Chen, and Aijun Du, “Single layer bismuth iodide: Computational exploration of structural, electrical, mechanical and optical properties,” [Scientific Reports](#) **5**, 17558 (2015)
- ⁵³ Jianwei Sun, Adrienn Ruzsinszky, and John P. Perdew, “Strongly constrained and appropriately normed semilocal density functional,” [Phys. Rev. Lett.](#) **115**, 036402 (2015)
- ⁵⁴ Hiroaki Ishizuka and Yukitoshi Motome, “Dirac half-metal in a triangular ferrimagnet,” [Phys. Rev. Lett.](#) **109**, 237207 (2012)
- ⁵⁵ Yuanchang Li, Damien West, Huaqing Huang, Jia Li, S. B. Zhang, and Wenhui Duan, “Theory of the dirac half metal and quantum anomalous hall effect in mn-intercalated epitaxial graphene,” [Phys. Rev. B](#) **92**, 201403 (2015)
- ⁵⁶ Pan Liu, Xiaoguang Luo, Yahui Cheng, Xue-Wei Wang, Weichao Wang and Hui Liu, Kyeongjae Cho, Wei-Hua Wang, and Feng Lu, “Physical realization of 2d spin liquid state by ab initio design and strain engineering in FeX_3 ,” [Journal of Physics: Condensed Matter](#) **30**, 325801 (2018)
- ⁵⁷ Indranil Rudra, Qin Wu, and Troy Van Voorhis, “Accurate magnetic exchange couplings in transition-metal complexes from constrained density-functional theory,” [The Journal of Chemical Physics](#) **124**, 024103 (2006)
- ⁵⁸ J. Strecka and M. Jascur, “A brief account of the Ising and Ising-like models: Mean-field, effective-field and exact results,” [Acta Physica Slovaca](#) **65**, 235–367 (2015)